ISSN-E: 2737-6419

Athenea Journal,
Vol. 4, Issue 13, (pp. 7-16)

https://doi.org/10.47460/athenea.v4i13.60

# Effects of thermoviscous flow and mechanical stresses on nitrogen desorption during iron transformation

Dam G. Oscar
https://orcid.org/ 0000-0002-0594-6757
oscar.curmetals@gmail.com
Unexpo, Vicerrectorado Puerto Ordaz
Puerto Ordaz-Venezuela

Received (3/06/2022), Accepted (27/08/2023)

**Abstract. -** The objective of this paper is a theoretical calculation of the mechanical stresses due to nitrogen pressure in an iron vacancy in the temperature range of 600 to 1100 °C and its effect on the swelling phenomenon associated with the high-temperature viscous flow. The method for quantification is theoretical and based on the analysis of experimental data reported in the literature. Two equations related to the variable were generated: swelling index with time and the stress due to nitrogen pressure. Both the variables are described in increasing ways and correlated significantly at the 99% confidence level. The equations include the value of stresses obtained from previous papers for ferrite (Feα) of 621, 2 Kgf/mm2 and for austenite (Feγ) of 727, 6 Kgf/mm2. The overall effect when opposing these values to the average sample cold compression strength of commercial samples, which varies with the corresponding degree of reduction, the final value of this parameter results in the range of 35.2 and 69.6 Kgf/mm2.

**Keywords:** Swelling, nitrogen, reduction, stresses.

## Efectos del flujo termoviscoso y de las tensiones mecánicas en la desorción de nitrógeno durante la transformación del hierro

**Resumen:** El objetivo de este trabajo es realizar un cálculo teórico de los esfuerzos mecánicos debidos a la presión de nitrógeno en una vacante de hierro en el rango de temperatura de 600 a 1100 °C y su efecto sobre el fenómeno de hinchamiento asociado al flujo viscoso a alta temperatura. El método de cuantificación es teórico basado en el análisis de datos experimentales reportados en la literatura. Se generaron dos ecuaciones que relacionan la variable índice de hinchamiento con el tiempo y con el estrés por presión de nitrógeno, en ambas las variables se relacionan de manera creciente y se correlacionan de manera significativa al 99% de confianza. Las ecuaciones incluyen el valor de tensiones, obtenido de trabajos anteriores, para ferrita (Feα) de 621,2 Kgf/mm2 y para austenita (Feγ) de 727,6 Kgf/mm2. El efecto global resultante al oponer estos valores al promedio de resistencia a la compresión en frío de las muestras comerciales, que varía con el correspondiente grado de reducción, da como resultado el valor final de este parámetro en el rango de 35.2 y 69.6 Kgf/mm2.

**Palabras clave:** Hinchamiento, nitrógeno, reducción, esfuerzos.

## I. INTRODUCTION

This investigation continues the swelling of iron oxides in metallization processes in the FeO/Fe phase transition [1]. In this theoretical work, a mechanism and a calculation method are defined to obtain the values of the pressure exerted by the absorption of nitrogen gas molecules. Consequently, the stresses generated by the desorption of three nitrogen gas molecules inside a point defect or vacancy of the crystal lattice need to be estimated in the presence of iron allotropic phases of ferritic (Feα) and austenitic (Feγ) iron at temperatures between 900 and 1100 °C, respectively, without quantifying thermoplastic effects on iron.

The objective is to calculate the stresses (pN2) and their relationship with the swelling phenomenon, incorporating the thermoplasticity characteristics of iron in the temperature range associated with the evolution from nascent iron to when the highest metallic iron content is obtained during the reduction process in the temperatures range 600 to 1100 °C. The following method was used for the purpose: (a) setting the temperature for the formation of iron; (b) calculations of the stress produced by nitrogen solubility in metallic iron described in the previous aimed temperature range [1], (c) fixing of temperature where iron acquires the thermoplastic property. Thus, apply the plasticity calculation method, determine the retention time at each reduction temperature, and associate the stress values with the swelling index (HI).

To quantify the values of the swelling index (HI) due to the expansion of dissolved nitrogen in a cluster of iron vacancies. It is (convenient) necessary to highlight that obtaining solid-state iron begins by reducing its minerals, oxides generally having fragile mechanical properties. The reduction progress starts with the increase in temperature and the presence of reducing agents; this process initiates metallic iron formation. The oxides and materials of known plastic properties at room and high temperatures present, and the viscous flow predominates; consequently, it is necessary to define these properties and relate them to the nascent iron. The thermoplastic property of iron will favor the participation of the abnormal swelling (HA) phenomenon if the stress produced by the pressure of nitrogen is greater than the yield stress and even more significant than the breaking stress. The value of the stresses previously obtained for Feα was 621.2 Kgf/mm2, and for Feγ, it was 727.6 Kgf/mm2. The criteria to incorporate and determine the start temperature of the thermoplastic effect of the metal is based on multiplying its melting temperature of the phases involved, FeO 1377ºC and 1535ºC for iron, by a specific proportionality factor, whose value varies depending on the source consulted.

## II. DEVELOPMENT

A. Fixing the nascent iron Nano crystal particle's temperature

In the reduction process of hematite iron oxide, with the increase in temperature, the well-known transformation to magnetite, wustite, and metallic iron occurs; this begins with the formation of Nanocrystals. After exceeding the critical radius, these will generate the nuclei and growth of iron Feα and become crystals, and to reach the cubic crystalline structure centered on the body, it is necessary to group at least nine atoms, two per cell with an edge of 0.33 nm. Thus, it turns out that the nascent iron is formed by Nanocrystals, consistent with experimental results obtained in [2] when iron nucleation is formed on wustite reduced with hydrogen at 800 °C and from a spheroidal nucleus with a diameter of 3.6 nm. The further growth of a pyramidal body with a square base with sides 4-8 nm and a height of 1.2-1.8 nm, as shown in Image 1 below determines the temperature at which the Nanocrystals appear. For this assessment, the Chaudron triple point of the iron-oxygen equilibrium diagram was used; this is the temperature point at which the magnetite/wustite/iron phases coexist simultaneously and, according to [3], is 590°C. For calculation purposes, a reference temperature of 600 °C was assumed.


**Fig. 1.** Semi-reduced natural ore particle reduced with 100% hydrogen, showing wustite (light gray) and several metallic iron nuclei on the wustite surface.
Source: Author files.

B. Stress calculations in iron allotropic phases

Following the proposed calculation methodology to determine the pressure of three nitrogen molecules in the vacancy of the iron crystal lattice, without considering thermoplastic effects, used in [1], and starting from 600 °C, the stress values were obtained, as shown in Table 1. It also got the relationship with the value of resistance to rupture of the allotropic phases of iron at room temperature; the obtained values are 28 and 105 Kgf/mm2 for Feα and Feγ, respectively.

**Table 1.** Stress produced by nitrogen in a vacancy of metallic iron in the study temperature range.

| Fe allotropic phase | Temperature (°C) | Stress (Kgf/mm$^2$) | Stress/Rupture Ratio |
|---|---|---|---|
| Feα | 600 | 462. 4 | 16.5 |
| Feα | 700 | 515.5 | 18.4 |
| Feα | 800 | 568.2 | 20.3 |
| Feα | 900 | 621.2 | 22.2 |
| Feγ | 1000 | 673.9 | 6.4 |
| Feγ | 1100 | 727.6 | 6.9 |

These stresses, knowing that they exceed the breaking strength of the iron, will be indirectly related to the expansion of the solid or agglomerate through the increase in the radius of the vacancy due to the thermoplastic effect that occurred in the material, depending on the time of agglomerate retention at each of the indicated temperatures.

The Nanocrystals generated at 600 °C will become crystals as the reduction process progresses and the temperature increases since most industrial reduction processes are carried out under dynamic, not isothermal, conditions.

C. High and low-temperature limits and the iron thermoplastic effect

The mechanical properties of materials are affected by temperature, specifically in crystalline solids such as metals and their alloys. Thus, the resistance properties of metals decrease with the increase in temperature, in exchange with the rise in plasticity properties and depending on the temperatures, stresses, and deformation speed. This can be achieved by the metal adopting a behavior quasi-viscous. It behaves like a fluid, increasing its original dimensions and limiting its use at high temperatures. In the criteria to determine the limits between low and high temperature, the correction factor is disclosed in [4], p. 373, and [5], p. 450, which is Tlow 0.5 and Thigh > 0.5 Tf. In an issue, it is considered to highlight that, in ferrous materials, the viscous flow begins at 420-430 °C, p.p. 355 and 429, respectively. It would correspond to a factor of 0.39, while in [6], p. 363, an aspect of 0.33 or 0.5 is considered, and in [7], p. 5, the plastic deformation starts from T > 0.6 Tf.

Thus, at high temperatures, it is necessary to consider the viscous flow due to hot forming or slow creep (Creep), as in the present work where the vacancy cavity is subjected to nitrogen pressure. When deformed at high temperatures, the material's response presents a curve similar to plastic flow at low temperatures. However, according to [6], these results do not allow predicting the behavior at high temperatures. However, in the temperature range studied for the FeO/Fe transformation, at 600 °C for nascent iron, it corresponds to the factor 0.48 (8), and for higher temperatures, values of 0.39 can be considered to 0.33, which is in the high-temperature range for the effects of thermoplasticity, viscous behavior.

To quantify the plasticity of iron at temperatures above 420 °C, equation (1) was used [9].

$$l = lo\,[1 + \beta\, t^{\frac{1}{3}}]e^{kt} \qquad (1)$$

l = Length of the material according to the time elapsed at the set temperature.
lo = Length at the instant of applying the effort.
β = Slope of strain rate, known as transient flow.
t = Time.
k = Slope of strain rate, called viscous flow.

According to [10], the parameters lo, β, and k are constants that must be determined experimentally since they correspond to physical processes, being necessary to obtain them to generate the curve that represents the thermoplastic characteristics of the material. In this regard, in his experimental results, p. 336, values of β and k are collected for iron, lead, copper, tin, and mercury at different temperatures. From their analysis, the following conclusions were highlighted:

- β, in general, presents slight variation with the increase in temperature, with a tendency to decrease.

- βFe, at a temperature of 444 °C (factor 0.40), although it increases with effort, tends to a constant value of 0.0210. When compared with the values of βPb, it presents a value of 0.045 at 17 °C, low temperature for Pb, and 0.043 at 160 °C (Thigh), associating it with the main result of his work, [10], p. 332, where he expresses "it is to show that typical metals of widely different natures obey the same general flow law," it is assumed that βFe will be maintained at high temperatures, that is, above 444 °C, so βFe = 0 will be used,0.0210.

- The value of k increases with the increase in temperature. With the effort to determine the values that it acquires at temperatures higher than 444 °C, it is necessary to know one of the following characteristics of iron: (a) the curve of real deformation (ε) as a function of the residence time at the temperatures previously set from 600 °C, (b) the constants indicated above for the same thermal range, data not available in the literature. Based on [4] "at elevated temperature viscous creep is predominant," p. 372; and the proof of it concerning k, p. 362, where it can be interpreted as independent of temperature, being consistent with results of viscous creep in aluminum, where a graph taken from [11] is shown showing the invariance of the relationship: ε = f(t), for absolute temperatures: 424, 478 and 531, p. 376, with factors 0.45, 0.46 and 0.57 respectively, the value of kFe = 0.00033 will be assumed. In the real case that it was more significant, an increase in stretching would be obtained with an increase in volumetric expansion, thus maintaining the accepted value of k, and a lower swelling index would be obtained.

D. Fixing the sample soaking time temperature range of 600 °C - 1100 °C

The sample soaking time will depend on the heating rate used in the reduction processes, whose values do not vary appreciably between them, as shown in Table 2, which summarizes the results of the best-known commercial processes.

**Table 2.** Heating rate according to industrial reduction processes.

| Process | Origin | Heating rate (°C/min) | Source |
|---|---|---|---|
| COREX | Experimental | 3.3 | [12] p. 16. Fig. 4.1.2.3. |
| HyL, Midrex | Oven design | 3.8 – 5.0 | [13] p.p. 87-91. |
| Blast furnace | Experimental | 5.0 | [14] |

The 5 °C/min rate will be used, considering that by applying the relationship (1), the length obtained for the 3.8 rates and 5 °C/min, a variation of 0.76 % is generated, that is, produces little impact, and also allows to be consistent with the search for greater productivity. For an increase of 100 °C, with a rate of 5 °C/min., the residence time equals 20 min. To associate the heating rate with the residence time of the material at temperatures between 600 and 1100 °C, heating bands were defined. A 100 °C increase in temperature would allow them to be associated with the retention time, and It accumulates as the temperature rises since the reduction process is continuous. Table 3 shows the results of this approach.

**Table 3.** Sample heating ranges, average temperatures, and retention time.

| Heating bands (°C) | Average temperature (°C) | Soaking time (min) | Heating bands (°C) | Average temperature (°C) | Soaking time (min) |
|---|---|---|---|---|---|
| 550-650 | 600 | 20 | 850-950 | 900 | 80 |
| 650-750 | 700 | 40 | 950-1050 | 1000 | 100 |
| 750-850 | 800 | 60 | 1050-1150 | 1100 | 120 |

## III. METHODOLOGY

The quantification method used is a theoretical approach, defined in the previous section, of a mechanism where the (a) physicochemical aspects of adsorption-desorption of nitrogen gas are associated, (b) crystalline structure of the material, (c) experimental data reported in the literature and (d) the ideal gas equation to facilitate algebraic calculations. For the study subjects, the phenomenon of abnormal swelling that can occur in the reduction of iron minerals in the solid state is included in the study, and through intentional sampling, six samples were fixed to relate the dependent variable (IH) with the reduction retention time and nitrogen pressure at a temperature of 600 to 1100°C.

Having defined the iron retention time at each average temperature, the expanded length is estimated by (1), considering the following values for the constants:

lo = initial length = vacancy radius of Fe crystal lattice: 0.124 nm.
β = 0.0210
k = 0.00033

## IV. RESULTS

A.Swelling Index relation with iron thermoplasticity

The resulting values of the expanded length make it possible to obtain the volume change concerning the initial volume of the vacancy left by an iron atom (8.0 10-3 nm3) and thus the swelling index (IH%), which will be associated with temperature and time and may be modeled dynamically. Results are shown In Table 4.

**Table 4.** According to residence time and temperature, the iron swelling index is associated with nitrogen pressure.

| Temperature (°C) | Retention time (min.) | Expanded length* (nm) | Expanded Volume x $10^{-3}$($nm^3$) | IH** (%) |
|---|---|---|---|---|
| 600 | 20 | 0,132 | 9,634 | 20,4 |
| 700 | 40 | 0,135 | 10,306 | 28,8 |
| 800 | 60 | 0,137 | 10,771 | 34,6 |
| 900 | 80 | 0,139 | 11,250 | 40,6 |
| 1000 | 100 | 0,141 | 11,742 | 46,7 |
| 1100 | 120 | 0,142 | 11,994 | 49,9 |

* Calculated (1). ** Obtenidos a través de Norma ISO 4698 [15].

B. Swelling index (HI) mathematical relationship with retention time

The dispersion graph is obtained through the Excel software, Fig. 1, with the regression line, dotted, and its equation (2) that allows estimating one variable from the other in the considered range and thus its correlation. This determines the degree of dependence between these variables in direction and magnitude, represented by the Pearson index (r). From the above data, it is possible to obtain a clear mathematical expression from the curves presented in Figure 1 and shown in Equation 2 for the estimation of the volume increase of an iron Nano crystallite.

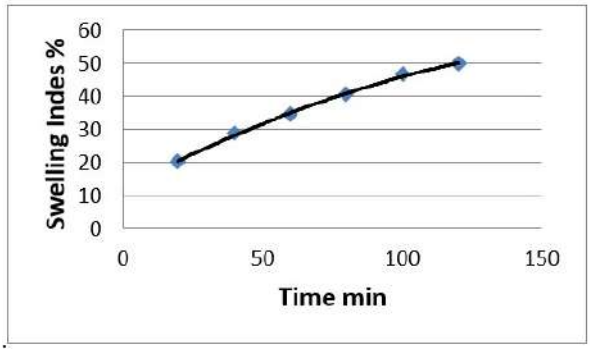


**Fig.2.** Retention/soaking time effect on the swelling index by iron induces thermoplasticity by partial pressure on N2 gas absorption desorption hysteresis.
Source: The author

$$IH\,(\%) = -0{,}0011\,t^2 + 0{,}451\,t + 11{,}98 \qquad R^2 = 0{,}998 \tag{2}$$

C. Mathematical relation between the swelling index and stresses due to the nitrogen pressure

In Table 1, it is shown that the stress generated by the nitrogen pressure in an iron vacancy exceeds the value of its resistance to breakage in a minimum ratio of 6.4 and a maximum of 22.2 times because this pressure increases the volume of the cavity depending on whether the thermoplastic response of the iron produces its rupture and gas escape, recovering the elastic deformation but not the plastic one, thus, utilizing the expanded volume, Table 4, the pressure is quantified through the procedure developed in [1], the values are recorded in Table 5.

**Table 5.** The swelling index in iron is associated with the effort generated by the nitrogen pressure.

| IH (%) | 20,4 | 28,8 | 34,6 | 40,6 | 46,7 | 49,9 |
|---|---|---|---|---|---|---|
| Stress (Kgf/mm$^2$) | 130,4 | 135,9 | 143,4 | 150,1 | 156,1 | 164,8 |

From the values in Table 5, a mathematical equation can be obtained through Figure 3 described in equation 3.

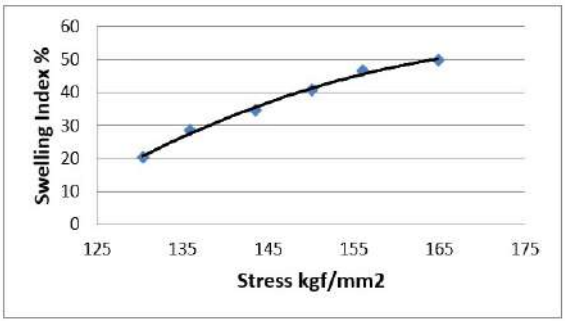


**Fig. 3.** Effect of the stress created by the nitrogen gas absorption on metallic iron on the final swelling index (percentage).
Source The author.

$$HI\ (\%) = -0{,}0126x^{*}\ 8kgf/mm2)^2 + 4{,}564^{*}\ (Kgf/mm2) - 360{,}46 \qquad (3)$$

At this stage, it is worth bearing in mind that the cold compression strength of manmade iron oxide agglomerates drops sharply with extended reduction time to 9 min; nevertheless, the compressive strength remained at the same level as that of 1 min. The reduction degree reached 11.11% at 1 min, corresponding to the magnetite phase, and finally increased to 32.45%rresponding to the wustite stage at 9 minutes. This effect is associated with the porosity increase and defect generation in the sample periphery, which causes strength loss [16]. The reduction step of hematite to magnetite causes the most extensive strength loss of 75.85% to approximately 200 Kgf/mm2, as shown in Fig. 4.

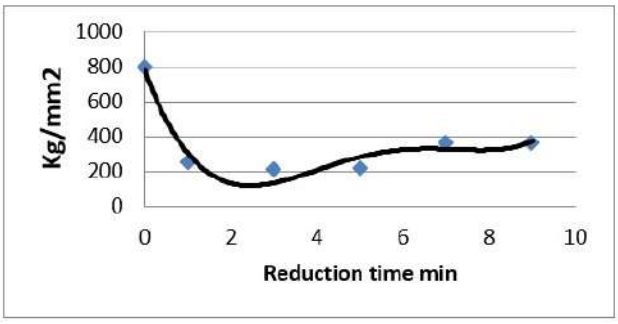


**Fig. 4.** Effect of reduction time on the compressive strength of iron aggregates in the transition from hematite to magnetite (16).
Edited by the author.

The effect shown in Fig. 4 can be represented mathematically by a polynomic equation shown in the polyphonic relationship in equation 4.

$$\textbf{Stress Kg/mm2 = 1.3583 t4 - 30.464 t3 + 234.82t2 - 681.12t + 777 } R^2 = 0.9395 \textbf{ (4)}$$

With these two expression stress values are presented in Table 5, and considering that it is an opposite vector working against the compression force that maintains the solid condition of the reduced sample obtained by equation 3, the resulting stress value may be in the range of 69.6 and 35.2 Kgf/mm2.

The mathematical findings in this research pay the importance of the strength of liquid-bound granules, which depend on at least three forces: (1) interparticle friction; (2) capillary and surface tension forces, supposed to be thermo creep of viscous FeO/Fe material, in the liquid between the nanoparticles; (3) viscous forces in the liquid between the particles. The former two have been addressed and quantified in this paper [17], [18].

The high correlations obtained in the equations of Figures 2 and 3 allow the association of the values with an increasing sense and a strong dependence between the variables. As in the present case, consider the correlation index robust due to the low dispersion between the values obtained and the regression line. Since the Pearson index does not give a cause-effect relationship, it is convenient to carry out a significance test. The test was done by comparing the statistical value (tc) of Student, calculated using (4) [19], p. 118, with the double-tailed tabulated value and degree of freedom (n-2), in the relationships: IH versus f(time) and IH versus f(pN2), with the null hypothesis Ho of "there is no correlation between the variables. "

$$tc = (|r| x \sqrt{(n-2)})/\sqrt{(1-r^2)} \quad (5)$$

The significance test result allowed us to reject the null hypothesis and accept a significant correlation with a confidence level of 99%. The relationships, IH versus f (time) and IH versus f(pN2), of Fig. 2 and 3, are consistent with the physical phenomenon of the reduction process. The former process involves the thermoplastic characteristics of both phases, considered FeO and iron, the time-temperature rise, and the expansive effect of the nitrogen pressure, which allows the assumption to be valid for the stress values presented in Table 5. These values, which are lower when compared with those of Table 2, were obtained without quantifying the expansive effect due to the thermoplasticity of iron. The data in Table 4 was used to establish the HI with the temperature variation relationship and obtain its linear regression and correlation.

## CONCLUSIONS

- This research has demonstrated and mathematically supported the triggering cause and effect of nitrogen's atomic absorption/molecular desorption in nascent iron nanoparticles during the wustite to iron reduction path.

- Including this effect reveals this gas as a hidden, and so far, disregarded, impurity, which triggers the abnormal swelling mechanism by inducing the internal mechanic stresses.

- The magnitude of the stresses generated by the nitrogen pressure in the iron crystal lattice and the mathematical relationship with the abnormal swelling index were determined. Considering the stresses act as a vector working against the compression force that maintains the solid condition of the reduced sample, it is possible to conclude that the value resulting from the stress is in the range of 69.6 and 35.2 Kg/mm2.

- From the laboratory and industrial analyzed data, a direct correlation was obtained between the partial pressure of nitrogen, the swelling index, and the reduction time.

- The obtained result indicates that the swelling index increases with the increase in the reduction temperature and that abnormal swelling, in the presence of Nitrogen gas, begins at 700 °C, reaching a maximum effect at 900ºC.

## ACKNOWLEDGEMENTS

The author would like to thank the Universidad Nacional Experimental Politecnica "Antonio Jose de Sucre" UNEXPO for their support in this research, as well as to Mr. Luis Alberto Azócar for carrying out the mathematical calculations and valuable suggestions on the definition of the defined swelling model.

## CONFLICTS OF INTEREST

The author declares no conflicts of interests

## REFERENCES

[1] L. A. Azócar. "Mecanismo de hinchamiento de óxidos de hierro en procesos de metallization". Athenea, vol. 3, no. 9, pp. 7-14, septiembre 2022. ISSN: 2737-6439. Doi: 10.47460/Athenea.
[2] T. Fujii, M. Hayashi, S. Oku, T. Watanabe, and K. Nagata. "Formation and growth of iron nuclei on wüstite surface at the initial stage of reduction." ISIJ International, vol. 54, no. 8, pp. 1765-1771, 2014.
[3] J. R. Gavarri and C. A. Carel, "Review about wüstite Fe1-zO, pseudo-phases, and defect clustering". Working document, February 2018, pp. 1-46. Institut Matériaux Microélectronique et Nano sciences de Provence, Université de Toulon, France.
[4] G. Dieter, "Metalurgia Mecánica", España: Aguilar, 1961
[5] G. Dieter, "Mechanical Metallurgy," Singapore: McGraw Hill International, 1988.
[6] J. F. Shackelford, "Ciencia de los materiales para ingenieros," (3° ed.) México: Prentice Hall Hispanoamericana. S. A., 1995.
[7] A. Al Omar, "Caracterización dinámica de dos aceros micro aleados de medio carbono mediante ensayos de compresión a alta temperatura aplicación de mapas de procesado", tesis doctoral. Ciencia de Materiales e Ingeniería e Metalúrgica. E. T. S. Barcelona, España: Universidad Politécnica de Catalunya. 1996.
[8] A. Echegaray, O. Dam G. Thermo viscosity mechanism approach in the formation of fayalite-type ceramic accumulations in particle separators in cfd reactors. In print Athenea.
[9] E. N da C. Andrade. "On the viscous flow in metals and allied phenomena." Proc. R. Soc. Lond. A, vol. 84, pp. 1-12, 1910.
[10] E. N da C. Andrade. "The flow in metals under large constant stresses." Proc. R. Soc. Lond. A, vol. 90, pp. 329-342, 1914.
[11] J. E. Dorn, "Creep and recovery," American Society for Metals. Metals Park. Ohio. 1957.
[12] T. I. Kang, "Study of reduction kinetics and properties of iron oxides for Corex process," Master of Science, Faculty of Science and Technology, University of New South Wales, Sydney. 2000.
[13] H. M. W. Delport, "The development of a DRI process for small-scale EAF-based steel mills," University of Stellenbosch, South Africa. 2010.
[14] A. Kasai and Y. Matsui, "Lowering thermal reserve zone temperature in Blast Furnace by adjoining carbonaceous material and iron ore," ISIJ International, vol. 44 no. 12, pp. 2073–2078, 2004.
[15] ISO 4698, "Iron ore pellets for blast furnace feedstocks-Determination of a free swelling index," Ginebra, ISO International Standard. 2007.
[16] Z. Huang, L. Yi, T. Jiang. Mechanisms of strength decrease in the initial reduction of iron ore oxide pellets. Powder Technology. Volume 221, May 2012, Pages 284-291.
[17] S.M. Iveson et al. Dynamic strength of liquid-bound granular materials: the effect of particle size and shape. Powder Technology, 2005.
[18] S.M. Iveson et al.The dynamic strength of partially saturated powder compacts: the effect of liquid properties. PowderTechnology. 2002.

[19] M. Miller and J. C. Miller, "Estadística y Quimiometría para Química Analítica", 4° ed. España: Prentice Hall, 2002.

**Oscar G. Dam**, a Metallurgical Engineer graduated from the Central University of Venezuela 1972. Master Science in Metallurgy and Diploma (DIC) Graduated from the Imperial College of Science and Technology 1977, England. PhD Engineering graduated from the University of London UK, 1983.